Three-Dimensional Structure of Leucocin A in Trifluoroethanol and Dodecylphosphocholine Micelles: Spatial Location of Residues Critical for Biological Activity in Type IIa Bacteriocins from Lactic Acid Bacteria[†,‡]

Nancy L. Fregeau Gallagher,[§] Miloslav Sailer,[§] Walter P. Niemczura,[||] Thomas T. Nakashima,[§] Michael E. Stiles,[⊥] and John C. Vederas*[,§]

Departments of Chemistry and Agricultural, Food, and Nutritional Science, University of Alberta, Edmonton, Alberta, Canada T6G 2G2, and Department of Chemistry, University of Hawaii, Honolulu, Hawaii 96822

Received May 28, 1997; Revised Manuscript Received September 9, 1997[⊗]

ABSTRACT: The first three-dimensional structure of a type IIa bacteriocin from lactic acid bacteria is reported. Complete ^{1}H resonance assignments of leucocin A, a 37 amino acid antimicrobial peptide isolated from the lactic acid bacterium *Leuconostoc gelidum* UAL187, were determined in 90% trifluoroethanol (TFE)−water and in aqueous dodecylphosphocholine (DPC) micelles (1:40 ratio of leucocin A:DPC) using two-dimensional NMR techniques (e.g., DQF-COSY, TOCSY, NOESY). Circular dichroism spectra, NMR chemical shift indices, amide hydrogen exchange rates, and long-range nuclear Overhauser effects indicate that leucocin A adopts a reasonably well defined structure in both TFE and DPC micelle environments but exists as a random coil in water or aqueous DMSO. Distance geometry and simulated annealing calculations were employed to generate structures for leucocin A in both lipophilic media. While some differences were noted between the structures calculated for the two different solvent systems, in both, the region encompassing residues 17−31 assumes an essentially identical amphiphilic α-helix conformation. A three-strand antiparallel β-sheet domain (residues 2−16), anchored by the disulfide bridge, is also observed in both media. In TFE, these two regions have a more defined relationship relative to each other, while, in DPC micelles, the C-terminus is folded back onto the α-helix. The implications of these structural features with regard to the antimicrobial mechanism of action and target recognition are discussed.

Lactic acid bacteria are the dominant natural microflora of many foods, including dairy products, fresh and processed meats, and fermented vegetables, where they inhibit the growth of harmful microorganisms on minimally processed refrigerated food products (Hoover & Steenson, 1993; Klaenhammer, 1993; Jack *et al.*, 1995; Stiles, 1996). Many of them produce bacteriocins, potent antimicrobial peptides which promise to be safe and effective food preservatives and possible replacements for nitrite in processed meats. These compounds also show considerable promise for other applications in human and animal health and may provide new approaches for dealing with antibiotic-resistant bacteria (Nissen-Meyer & Nes, 1997). Bacteriocins have been classified into four types (Klaenhammer, 1993). Type I bacteriocins such as nisin A (Jung & Sahl, 1991; Kuipers *et al.*, 1993; Engelke *et al.*, 1994), which is commercially employed for preservation of dairy products, are extensively posttranslationally modified. Others, with potential for use in meat, have no modifications except for cleavage of an N-terminal extension and, in some cases, formation of disulfide bridges. In the latter category, the 37 amino acid peptide leucocin A (LeuA; Hastings *et al.*, 1991, 1994; Stiles, 1994)[1,2] from *Leuconostoc gelidum* is one of a rapidly expanding group (type IIa) of hydrophobic bacteriocins that contain a YGNGV amino acid motif near the N-terminus (Figure 1).

Shortly after the primary sequence of LeuA was elucidated (Hastings *et al.*, 1991), mesentericin Y105 (Mes) was isolated from *Leuconostoc mesenteroides* (Héchard *et al.*, 1992; Fremaux *et al.*, 1995). Mes differs from LeuA only at two sites (Fremaux *et al.*, 1995; Fleury *et al.*, 1996); it has an alanine substituted for Phe22 and contains an isoleucine in place of Val26.[3] Other class IIa bacteriocins with very similar N-terminal sequences include carnobacteriocin B2 (Quadri *et al.*, 1994), sakacin A (also called curvacin A; Holck *et al.*, 1992; Ticheczek *et al.*, 1993), sakacin P (also

[†] These investigations were supported by the Natural Sciences and Engineering Research Council of Canada.

[‡] Coordinates of leucocin A in TFE and DPC micelles have been deposited in the Brookhaven Protein Data Bank (filenames 2leu and 3leu, respectively).

[§] Department of Chemistry, University of Alberta.

[||] Department of Chemistry, University of Hawaii.

[⊥] Department of Agricultural, Food, and Nutritional Science, University of Alberta.

[⊗] Abstract published in *Advance ACS Abstracts,* November 15, 1997.

[1] Abbreviations: CD, circular dichroism; CO, backbone carbonyl carbon; CSI, chemical shift index; $d_{\alpha N}(i,j)$, distance and corresponding NOE connectivity between H_α and HN of residues *i* and *j*, respectively; $d_{\beta N}(i,j)$, distance and corresponding NOE connectivity between H_β and HN of residues *i* and *j*; $d_{NN}(i,j)$, distance and corresponding NOE connectivity between HNs of residues *i* and *j*, respectively; DMSO, dimethyl sulfoxide; DPC, dodecylphosphocholine; DQF-COSY, double-quantum-filtered correlation spectroscopy; DSS, 2,2-dimethyl-2-silapentane-5-sulfonic acid; H_α, α proton; H_β, β proton; HN, backbone amide proton; HPLC, high-pressure liquid chromatography; LeuA, leucocin A; MeCN, acetonitrile; Mes, mesentericin Y105; NMR, nuclear magnetic resonance; NOE, nuclear Overhauser effect; NOESY, 2D NOE spectroscopy; RMSD, root mean square deviation; TFA, trifluoroacetic acid; TFE, trifluoroethanol; TOCSY, total correlation spectroscopy.

[2] Recently, the structural gene of leucocin B from *Leuconostoc carnosum* Ta11a was determined and shown to code for a mature bacteriocin with the same sequence as LeuA, but a 24 amino acid leader peptide at the N-terminus of its precursor differs from that of LeuA by seven residues (Felix *et al.*, 1994).

S0006-2960(97)01263-4 CCC: $14.00

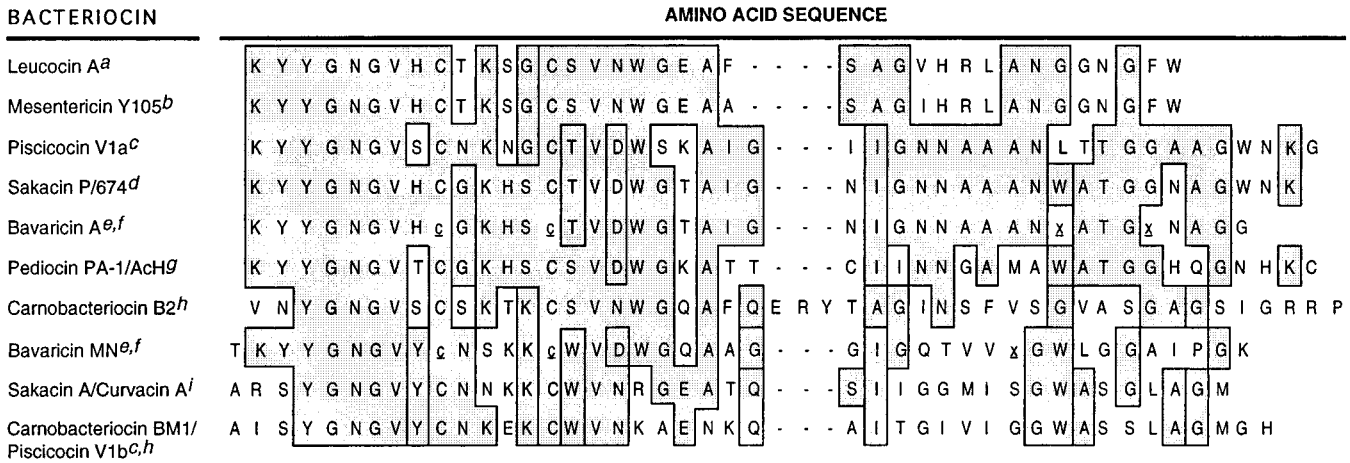

FIGURE 1: Amino acid sequences of YGNGV bacteriocins aligned for the best overlap. The boxes outline conserved residues. Footnotes: [a]Hastings *et al.*, 1991. [b]Fremaux *et al.*, 1995; Fleury *et al.*, 1996. [c]Bhugaloo-Vialet *et al.*, 1996. [d]Tichaczek *et al.*, 1994; Holck *et al.*, 1994. [e]Kaiser & Montville, 1996. [f]c and x represent amino acids which were not fully verified. [g]Manugg et al., 1992; Bukhtiyarova et al., 1994. [h]Cuadri et al., 1994. [i]Holck et al., 1992; Ticheczek et al., 1993.

called sakacin 674; Ticheczek *et al.*, 1994; Holck *et al.*, 1994), pediocin PA-1 (also called pediocin AcH; Marugg *et al.*, 1992, Bukhtiyarova *et al.*, 1994), bavaricins A and MN (Kaiser & Montville, 1996), carnobacteriocin BM1 (also called piscicocin V1b; Quadri *et al.*, 1994; Bhugaloo-Vial *et al.*, 1996), and piscicocin V1a (Bhugaloo-Vial *et al.*, 1996). Despite large regions of sequence identity and close homology in the N-terminal 22 residues, these bacteriocins display considerable disparity in the spectra of antimicrobial activity. This suggests that detailed knowledge of their three-dimensional structures is vital to understanding their mode of action as well as resistance to their antimicrobial effects.

We have recently characterized the genes involved in the production of LeuA (Hastings *et al.*, 1991; van Belkum & Stiles, 1995). The gene *lcaA* encodes a 61 amino acid peptide identified as LeuA with a 24-residue N-terminal extension that is essential for secretion by an ABC transporter (van Belkum *et al.*, 1997). This is followed by *lcaB*, the gene for the 113 amino acid protein which is required for immunity to LeuA. On the strand opposite to these two genes and upstream of them, three more open reading frames were observed: *lcaC*, *lcaD*, and *lcaE*. These code for an ATP-binding cassette (ABC) transporter, another gene essential for LeuA production and a third protein of unknown function, respectively. We have also isolated a 111 amino acid protein, CbiB2, from *Carnobacterium piscicola*; when expressed in cells, this protein confers immunity to the closely related peptide, carnobacteriocin B2 (Quadri *et al.*, 1994, 1995), but its mechanism of operation is presently unknown. Interestingly, it does not confer immunity to the closely related and coproduced carnobacteriocin BM1, which requires its own specific immunity protein (Quadri *et al.*, 1995). The plasmid encoding a homologous bacteriocin, pediocin AcH, in *Pediococcus acidilactici* also contains a structural gene for an analogous 112 amino acid immunity protein (Motlagh *et al.*, 1994).

Like many other antibacterial peptides (Saberwal & Nagaraj, 1994; Nissen-Meyer & Nes, 1997), the type IIa bacteriocins from lactic acid bacteria are believed to act at the membrane of target organisms, probably by binding to an unidentified protein receptor, to cause leakage of cellular contents (van Belkum *et al.*, 1991; Maftah *et al.*, 1993; Bruno & Montville, 1993; Chikindas *et al.*, 1993; Christensen & Hutkins, 1994; Montville & Bruno, 1994; Abee, 1995a). Recently, a number of proposals have been published suggesting possible orientations of bacteriocins (and in some cases their putative receptors) in lipid bilayers (Bhugaloo-Vial *et al.*, 1996; Fleury *et al.*, 1996; Franke *et al.*, 1996; Chen *et al.*, 1997), but no three-dimensional structures based on NMR spectrometry or crystallographic studies have yet been reported.[4]

Our initial NMR investigations have shown that LeuA exists as a random coil structure in water and DMSO (Henkel *et al.*, 1992; Sailer *et al.*, 1993). It is well established that solvents such as trifluoroethanol (TFE; Waterhous & Johnson, 1994; Jasanoff & Fersht, 1994) and dodecylphosphocholine (DPC) micelles (Brown & Wüthrich, 1981; Wider *et al.*, 1982; Inagaki *et al.*, 1989; Karslake *et al.*, 1990; Macquaire *et al.*, 1992; Constantine *et al.*, 1993; Kallick, 1993; Thornton & Gorenstein, 1994) can induce defined conformations in small peptides which normally exhibit no stable secondary structure in aqueous solution. These mixed solvent systems, because of their dual lipophilic and aqueous nature, may also stabilize structures that more closely approximate the biologically relevant conformations of protein-bound molecules (Waterhous & Johnson, 1994). A number of studies suggest that peptides acting on membrane-bound protein receptors encounter the lipid membrane before interacting with the receptor (Moroder *et al.*, 1993; Schwyzer, 1995). The lipid membrane may assist receptor binding by locking the peptide into its bioactive shape and thereby changing the conformational search from a three-dimensional to a two-dimensional process (Tessmer & Kallick, 1997, and references therein). Hydrophobic peptides such as LeuA are difficult to crystallize for X-ray studies and tend to self-aggregate at higher

[3] It was initially reported (Héchard *et al.*, 1992) that Mes also lacked the C-terminal tryptophan and displayed a quite different spectrum of antimicrobial activity. However, this has been corrected (Fremaux *et al.*, 1995), and a recent study (Fleury *et al.*, 1996) demonstrates that there are only slight differences in the bioactivity of Mes and LeuA against a variety of microorganisms unless the terminal Trp37 residue of Mes is removed, which drastically decreases its antimicrobial properties.

[4] The lantibiotic nisin A, which is extensively posttranslationally modified, undergoes structural transitions in nonaqueous environments. Its structures in two different lipophilic environments have recently been elucidated (van den Hooven *et al.*, 1993, 1996).

concentrations. Fortunately, the modern multidimensional NMR techniques available for complete assignment of protein resonances (Roberts, 1993; Leopold *et al.*, 1994; Bax, 1994; Edison *et al.*, 1994; Wüthrich, 1986) and determination of long-range NOEs allow analysis of the three-dimensional structure of such compounds.

In the present study, we compare the complete resonance assignments and calculated three-dimensional structures of LeuA in TFE and DPC micelles. These structures provide an essential framework for a molecular level understanding of the mechanism by which bacteriocins exert their antimicrobial activity, the specificity of their action, and the function of their immunity proteins. Comparison of leucocin A with known sequences of other type IIa bacteriocins suggests common structural themes that may play key roles in interaction with the putative receptor proteins in target cells.

MATERIALS AND METHODS

Production and Isolation of Leucocin A. The procedures previously reported (Hastings *et al.*, 1991; Henkel *et al.*, 1992; Sailer *et al.*, 1993) for fermentation of *L. gelidum* and for purification of LeuA were slightly modified. Five liters of medium containing (per liter) casamino acids (15 g), yeast extract (5 g), glucose (25 g), $K_2HPO_4 \cdot 3H_2O$ (1 g), $MgSO_4$ (0.1 g), $MnSO_4 \cdot 4H_2O$ (0.05 g), and Tween 80 (1 mL) was inoculated with 150 mL of a 12-hour-old culture of *L. gelidum* UAL187. The fermentation broth was gently stirred for 28 h under N_2 atmosphere at 24 °C, and the pH was maintained at 6.2 with a pH controller (Chem-Cadet, Cole-Palmer) by addition of 2 M NaOH (total 220 mL). The cells were removed by centrifugation, and the supernatant was loaded directly onto an Amberlite XAD-8 (BDH Chemicals) column (4.5 × 50 cm) preequilibrated with 0.1% aqueous trifluoroacetic acid (TFA) and sequentially washed with increasing concentrations of ethanol (2 L of each of 0, 20, and 35%; 1.5 L of 50%; and 1 L of 80%). The most active fraction (50% ethanol) having 75% of the antimicrobial activity (determined against the indicator strain *Carnobacteriocin divergens* LV13) was concentrated *in vacuo* at 30 °C to 15 mL. It was then mixed with an equivalent volume of MeCN and applied onto a Sephadex LH-60 (Sigma) column (5 × 25 cm) equilibrated with 50% aqueous MeCN containing 0.1% TFA. The bioactive fractions were pooled and concentrated to 20 mL. The final purification was accomplished by HPLC with a Waters μ-Bondapak RP-18 column (25 × 200 mm, 15 μm, 125 Å, monitored at 220 nm, flow rate 10 mL/min) using a gradient from 32% to 35% MeCN in 0.1% aqueous TFA and, subsequently, an isocratic elution with 34% MeCN in 0.1% TFA. A total of 40 mg of pure LeuA was obtained. Purity was confirmed by HPLC and electrospray mass spectroscopy as described previously (Hastings *et al.*, 1991).

CD Spectroscopy. All measurements were made by Mr. Kim Oikawa (Biochemistry Department, University of Alberta) on a Jesco 720 spectrometer in a 0.02 cm cell at concentrations of 0−90% TFE in 0.1% aqueous TFA over 180−255 nm. The concentration of LeuA was 0.25 mM. Corresponding experiments were done using DPC micelles in water containing 0.1% TFA by varying the ratio of LeuA to DPC from 1:0 to 1:40.

NMR Sample Preparation. LeuA samples were dissolved either in 550 μL of TFE-d_3/H_2O, 9:1 (v/v), or in a 180 mM solution of perdeuterated dodecylphosphocholine (DPC) with 10% D_2O and then sonicated for 1 min with a Cole-Palmer sonicator under N_2 atmosphere to give a total concentration 4.5 mM. TFE-d_3 was 99.94% deuterated (Cambridge Isotopes, Andover, MA) and DPC-d_{38} was 99.4% deuterated. The latter material was generously provided by Dr. Laird Trimble of Merck Frosst Ltd. (Pointe Claire, Quebec). All samples were acidified (pH 2.8, uncorrected) by adding TFA (0.1% final concentration) or CF_3COOD (for proton exchange experiments).

NMR Spectroscopy. The LeuA spectra were recorded on a Varian Unity 500 NMR spectrometer operating at a proton frequency of 500 MHz. All experiments in 90% TFE solution were done at 26 °C with a sweep width of 5300 Hz. The residual signal from protonated TFE was used as the reference [3.88 ppm downfield from 2,2-dimethyl-2-silapentane-5-sulfonic acid (DSS)]. Spectra in DPC micelles were recorded at 35 °C with a sweep width of 6000 Hz and referenced to external DSS at 0 ppm. Water suppression was obtained by continuous irradiation of the partially deuterated water signal at all times except during data acquisition. DQF-COSY (Rance *et al.*, 1983) were done essentially as described previously for LeuA in water and DMSO solutions (Sailer *et al.*, 1993). Two-dimensional total correlation spectroscopy (TOCSY; Griesinger *et al.*, 1988) and nuclear Overhauser effect spectroscopy (NOESY; Roberts, 1993; Jeener *et al.*, 1979) were employed to obtain sequential resonance assignments and NOE patterns. All spectral data were collected with 256−512 increments in the t_1 dimension, 2048 complex data points in t_2, 32−64 scans, and a relaxation delay typically between 1.6 and 2 s. Mixing times of 100, 150, and 250 ms for the NOESY and 30−75 ms for the TOCSY experiments were used. Prior to Fourier transformation, the data matrix was zero-filled to 2K × 2K complex points and multiplied by a sine bell or Gaussian window function. Amide deuterium (proton) exchange ratios were monitored by recording one-dimensional spectra at different times. To distinguish overlapping signals as well as to determine the relative NH exchange rates, additional NOESY spectra were recorded after 1, 3, 12, 24, and 48 h.

NMR Restraints and Structure Calculations. Distance constraints were determined by volume integration of correlations observed in NOESY spectra with 150 ms mixing times using the VNMR software (Varian Associates, Palo Alto, CA). NOEs with other mixing times mentioned above were used to make or confirm chemical shift assignments and to check for spin diffusion. NOESY spectra were first corrected for baseline distortions. For spectra acquired in TFE, the NOEs were categorized as strong, medium, or weak, and the corresponding distance restraints were assigned as having upper limits 2.5, 3.3, and 5.0 Å, respectively. For spectra acquired in DPC micelles, four classifications were used with upper bounds of 2.5, 3.2, 4.0, and 5.0 Å. In all cases, the lower bound was defined as the sum of the van der Waals radii of the two atoms involved in the restraint. In some instances, a cross peak could not be unambiguously assigned. Such NOEs were included as overlapping NOE distance restraints, in which case a weighted average of all of the distances which comprise the restraint was used in the calculation of the structures. A force constant of 10 kcal/mol was used to enforce all distance restraints.

Eight hydrogen bond restraints (CO_i−HN_{i+4}, range 1.8−2.2 Å) were also included in the calculation of the structures

in both solvents. These were determined on the basis of slowly exchanging amide protons and the pattern of NOEs characteristic of an α-helix. Pseudoatoms were used for all nonstereospecifically assigned protons and appropriate corrections added to the restraints. All prochiral constituents which could be distinguished spectroscopically were initially treated as floating pairs.

Structures of LeuA in TFE and DPC micelles were calculated using DGII [Molecular Simulations, Inc., San Diego, CA, a distance geometry/simulated annealing program (Havel, 1991)]. The consistent-valence force field (CVFF; Dauber-Osguthorpe *et al.*, 1988) was used for the structure refinement. The starting structure was built as an extended conformation with all ionizable groups protonated. This structure was then subjected to triangle inequality bound smoothing and embedded in four dimensions, using prospective metrization and majorization with a constant weighting scheme. The structures thus calculated were then optimized by simulated annealing using an initial upper bound on the temperature of 200 K, an initial energy of 1200 kcal/mol, a step size of 0.3 ps, and atomic masses of 1000 Da for 15 000 (TFE) or 20 000 (DPC micelles) steps. This was followed by 400 steps of conjugate gradient minimization.

A refinement process was implemented by examining the distance violations of the resulting structures for consistent, large violations of a given restraint or a set of restraints that clustered around a specific residue. Such violations generally occurred for correlations involving strongly coupled protons (e.g., geminal) for which the size of the NOEs was distorted by spin diffusion, resulting in an underestimate of the true distances. In such instances, the upper bound of the relevant restraint was relaxed to the next lower classification or removed completely. In addition, for LeuA in DPC micelles, five prochiral pairs were stereospecifically assigned by determining which assignments caused consistent violations of restraints. Analysis of the structures for LeuA in DPC micelles also allowed the resolution of several ambiguous restraints. After these adjustments were made to the restraints, a new set of structures was calculated by the above procedure. This process was repeated in an iterative fashion until the final set of structures was judged to be well converged.

For LeuA in TFE, 20 structures were produced in the final calculation of which the best 18 were selected. For LeuA in DPC micelles, the final calculation resulted in 25 structures of which the best 19 were selected. In both cases, the other structures were discarded because they had maximum distance violations greater than 0.25 Å and RMSDs from distance restraints greater than 0.15 Å. For the final calculation of the conformers of LeuA in TFE, a total of 398 NOE distance (155 intraresidue, 118 sequential, 89 medium range, and 36 long range), 22 overlapped NOE distance, 30 chiral, and 8 hydrogen bond restraints were used. For the final calculation of the conformers of LeuA in DPC micelles, a total of 338 NOE distance (137 intraresidue, 119 sequential, 69 medium range, and 13 long range), 14 overlapped NOE distance, 30 chiral, and 8 hydrogen bond restraints were used. The coordinate files for LeuA in TFE and DPC have been deposited in the Brookhaven Protein Data Bank (filenames 2leu and 3leu, respectively).

RESULTS

CD and NMR Spectra of Leucocin A. In order to determine optimal conditions for NMR studies, CD spectra of LeuA were first acquired at various concentrations of TFE or DPC in water. Randomly coiled or partially structured polypeptides are known to show observable transitions to α-helical forms as the TFE concentration increases (Waterhous & Johnson, 1994; Jasanoff & Fersht, 1994). Since LeuA is relatively unstable under basic conditions (Hastings *et al.*, 1991), 0.1% trifluoroacetic acid was added to solutions in all experiments. The CD spectra (data not shown) of solutions of LeuA (1.0 mg/mL) indicate transition to a conformation with significant α-helical content at higher concentrations of TFE (>30%) (Brahms & Brahms, 1980; Chang *et al.*, 1978). The α-helical content continued to increase up to the maximum amount of TFE used (90%). Similar experiments in DPC micelles suggest analogous structural changes with a solvent system having a 40:1 ratio of DPC:LeuA in water (with 0.1% trifluoroacetic acid), an environment previously found to be optimal for inducing secondary structure in a mitochondrial signal peptide (Karslake *et al.*, 1990). Hence, to maximize the opportunity for observation of defined structure, the present NMR studies of LeuA use 90% aqueous TFE and such DPC micelles (with 0.1% trifluoroacetic acid in both cases).

The application of NMR spectral techniques and strategies previously employed (Henkel *et al.*, 1992; Sailer *et al.*, 1993) to assign the spectra of LeuA in water and DMSO (i.e., DQF-COSY, TOCSY, and NOESY) permit reassignment of the ^{1}H NMR spectra in 90% TFE in water and in DPC micelles. However, for the present work the sample is not labeled with ^{13}C or ^{15}N. The chemical shifts of the α-hydrogen (H_α) of each amino acid residue in both solvent systems can be compared against the corresponding shifts in water/DMSO (9:1; Sailer *et al.*, 1993) and literature values (Wüthrich, 1986; Wishart & Sykes, 1994) for the identical residues in random coil peptides. In each solvent, the presence of the disulfide bridge imposes considerable local structure that leads to downfield shift of the α-proton resonance positions for nearby residues (data not shown). However, in water/DMSO, the chemical shifts of the C-terminal half of the peptide chain (residues 17−37) do not vary significantly from those seen in random coils. In contrast, in both the TFE and DPC systems, the H_α of residues 18−30 are shifted upfield from random coil values.

This can be clearly demonstrated by the use of the chemical shift index developed by Wishart and Sykes (Figure 2; Wishart & Sykes, 1994). This technique employs a comparison of the chemical shifts of H_α to a set of empirically determined ranges. A value of +1 is assigned to those residues which are downfield of the index, −1 for upfield chemical shifts, and 0 for those within the range. A local "density" of more than 70% of +1 values indicates a region of β-strand, while a similar grouping of −1 values denotes an α-helix. No correction was made for the intrinsic effect of TFE on the chemical shifts not related to structural change, but these effects have been found to be insignificant for H_α (Merutka *et al.*, 1995). Figure 2 shows that LeuA in both TFE and DPC micelles has a β-sheet structure between residues 6 and 16, the region containing the disulfide bridge, which is interrupted by a turn at residues 11 and 12. Following this β-sheet loop is an α-helix (residues 18−30).

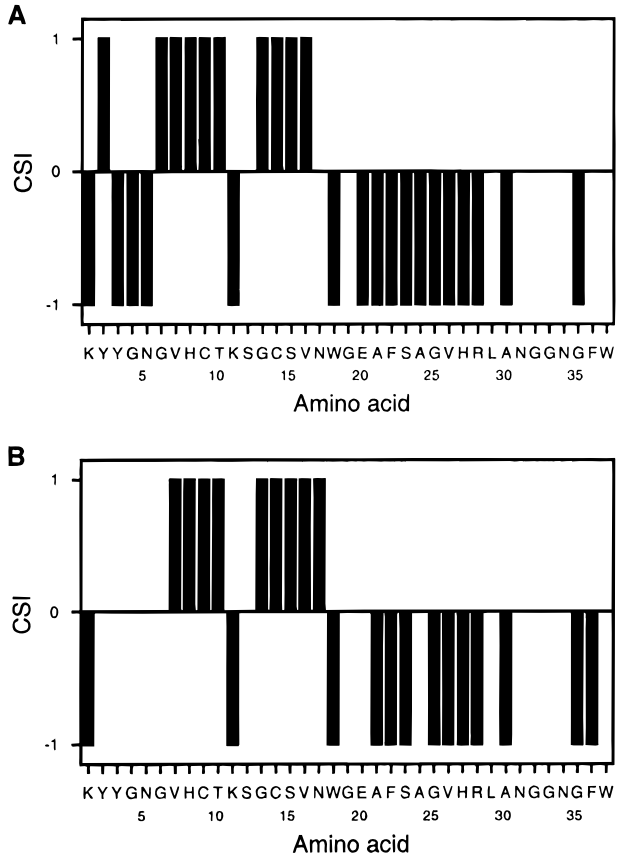

FIGURE 2: Chemical shift index (CSI; Wishart & Sykes, 1994) versus residue number for the H_α of LeuA in (A) TFE and (B) DPC micelles. A local density of more than 70% of −1 values indicates a region of α-helix, while such a grouping of +1 values denotes a β-sheet.

Long-range NOEs are essentially absent in spectra of LeuA in water/DMSO solvent systems except for some interactions in the disulfide loop region (Henkel *et al.*, 1992; Sailer *et al.*, 1993), as would be expected for random coil peptides. However, they are abundant in the TFE and DPC media and provide the key information for distance geometry calculations and modeling of the three-dimensional structures. A typical section of the NOESY spectra showing the NH to H_α ($d_{\alpha N}$) interactions in TFE, as well as some other long-range correlations, is given in Figure 3A. In this fingerprint region, there is extensive overlap due to the large number of glycine residues. Nevertheless, the spin systems can be established through analysis of TOCSY spectra, and the NOESY spectra identify essentially all sequential connectivities for adjacent residues [$d_{NN}(i,i+1)$, $d_{\alpha N}(i,i+1)$, and $d_{\beta N}(i,i+1)$] (Figure 4). Spectra obtained during proton−deuterium exchange experiments support these assignments. A number of amino acids in the C-terminal half of LeuA show a number of medium-range interresidue NOEs (Figures 3A and 4). These include $d_{NN}(i,i+2)$, $d_{\alpha N}(i,i+3)$, $d_{\alpha\beta}(i,i+3)$, and $d_{\alpha N}(i,i+4)$ from Asn17 through Asn31 which are typical for α-helical structures.

Many of the residues in the N-terminal half also show medium- and long-range NOEs as summarized in Figure 4 (e.g., Tyr2 H_α to His8 H_α, Tyr3 HN to His8 H_α, Val7 H_α to Asn17 HN, His8 HN to Val16 H_α, Cys9 H_α to Cys14 H_α, Thr 10 HN to Cys14 H_α, and Thr10 H_α to Ser12 HN in Figure 3A). These NOEs indicate that this region forms an antiparallel β-sheet around the disulfide bridge (Cys9 to Cys14) with a β-turn between Thr10 and Gly13. Another β-turn can be observed between Gly4 and Val7 preceded by a third strand of the β-sheet. Thus the β-sheet region extends from the N-terminus to Val16. Three NOEs connecting the β-sheet region to the α-helix are also observed. NOEs between the H_α of Asn5 and the methyl groups of both Ala21 and Ala24, as well as between the aromatic protons of Tyr2 and the H_β of Glu20, indicate that in TFE the β-sheet region folds over onto the α-helix. No medium- or long-range NOEs are observed for residues 32−37, suggesting that this region exists as a random coil.

The assignment of LeuA in DPC proceeded analogously to that in TFE with alignment of the spin systems, established by DQF-COSY and TOCSY spectra, with the primary sequence using NOESY spectra. All NH to NH sequential connectivities (d_{NN}) could be established except for a few interruptions due to spectral overlap. These were overcome using $d_{\alpha N}$ and $d_{\beta N}$ interactions. The NH to NH portion of the NOESY spectrum of LeuA in DPC micelles is depicted in Figure 3B. As in TFE, long-range correlations (Figure 4) identify an α-helical structure for the C-terminal half of the peptide, in this case from Trp18 to Gly32. The overall pattern of NOEs for the N-terminal domain is similar to that observed in TFE, but fewer NOEs are present in this region in DPC micelles, suggesting that this portion of the molecule is less defined in this medium. Unlike in TFE, LeuA in DPC micelles shows little indication of how the α-helix is oriented relative to the β-sheet. The only relevant correlation is that one of the methyl groups of Val16 exhibits a moderately strong NOE to the methyl group of Ala21. However, a few new long-range NOEs are observed. A methyl group on Val26 displays a weak NOE to one of the aromatic protons on Phe36, suggesting that the C-terminus folds back onto the α-helix. Other potential connections between this methyl group and the end of the peptide chain are correlations observed between it and protons at 7.27 and 7.12 ppm. Neither of these protons could be unambiguously assigned. The former corresponds to either an aromatic proton on Phe22 or Trp37, while the latter is attributed to an aromatic proton on either Phe36 or Trp37.

The unusually high (upfield) shift of the amide hydrogen of Gly4 (5.42 ppm) in TFE is due to the shielding effect of the neighboring aromatic ring of Tyr2. A similar effect is seen for one of the α protons on the same glycine residue which appears at 3.31 ppm. In DPC micelles, this aromatic ring is oriented away from the backbone of subsequent residues, resulting in more typical chemical shifts for the HN and H_αs of Gly4 (7.49, 3.98, and 3.80 ppm, respectively). In TFE, and especially in DPC micelles, extensive line broadening occurs (Thornton *et al.*, 1993) which hinders measurement of spin−spin coupling constants, which are another criterion for the presence of secondary structure.

Hydrogen Exchange Experiments. Amide hydrogen exchange experiments in both TFE and DPC environments using D_2O demonstrate that most such protons are completely exchanged within 3 h except for a few which remain unequilibrated with solvent for up to 2 days. Analysis of NOESY spectra of these samples and of complementary experiments in which predeuterated LeuA is treated with H_2O confirms the assignments and overcomes problems of spectral overlap. The relative rates of exchange are indicated in Figure 4. Both the D for H and H for D exchange studies show that residues in the Gly19 to Leu29 region of the peptide in both TFE and DPC media exchange their amide

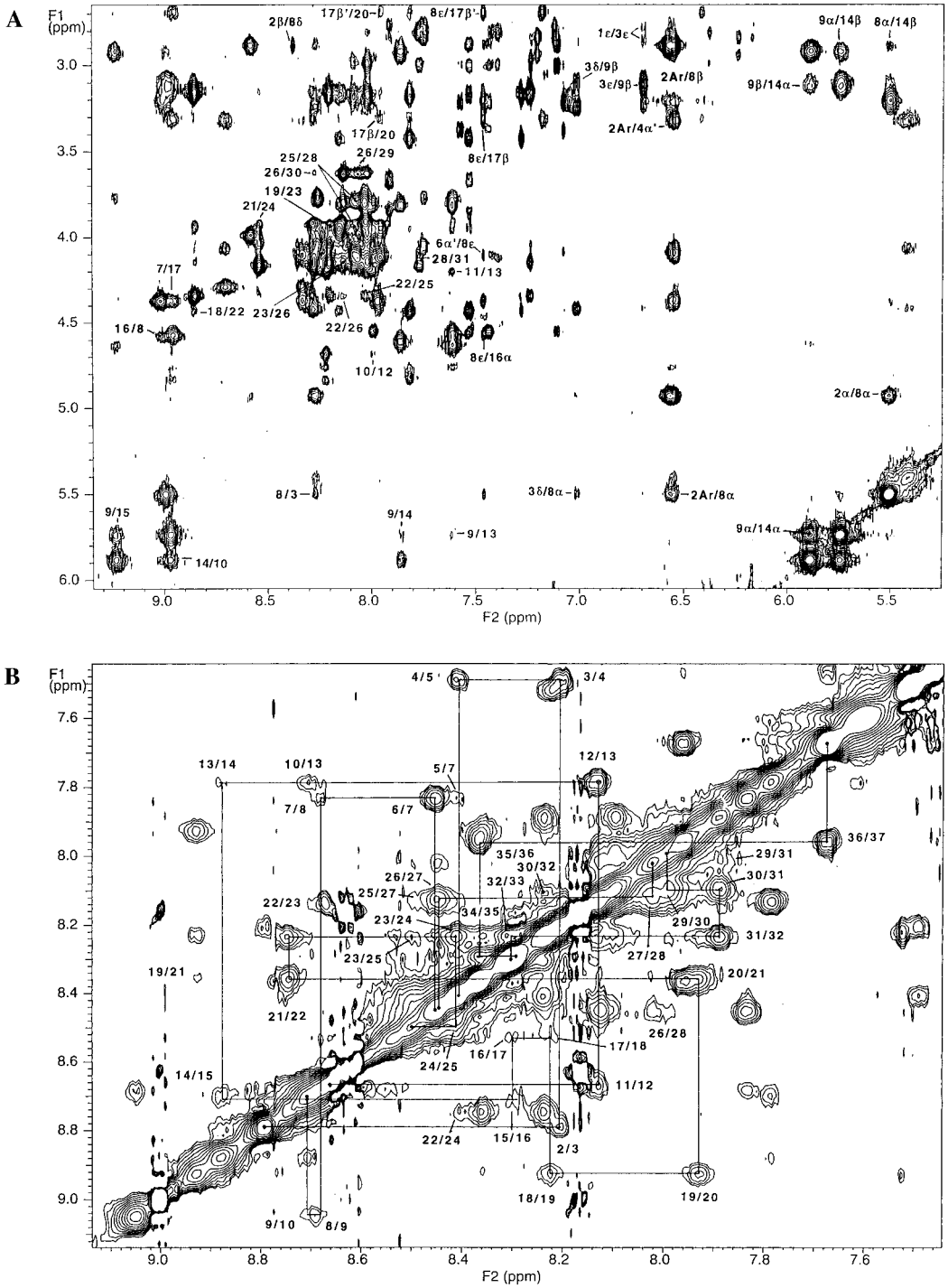

FIGURE 3: Enlargements of NOESY spectra (150 ms mixing time) of LeuA with selected interactions labeled for (A) the HN to H_α region in 90% TFE (unless otherwise indicated) and (B) the HN to HN region in DPC micelles with the sequential connectivity indicated by the solid line.

protons slowly, suggesting that they are shielded from the water in the bulk solution, consistent with a defined α-helix structure in this part of the molecule. In TFE, several of the NHs in the latter part of the β-sheet domain also show slow exchange rates, suggesting, as did the NOE results described above, that this region is better defined in this solvent than in DPC micelles.

Three-Dimensional Structure. The distance geometry calculations employ constraints obtained from analyses of NOESY spectra in the TFE or DPC environments. The restraints originate from classification of NOESY cross peak intensities into three or four categories based on integration (upper bounds for TFE, 2.5, 3.3, and 5.0 Å; upper bounds for DPC, 2.5, 3.2, 4.0, and 5.0 Å). A total of 398 NOEs (including 125 medium- and long-range NOEs) for LeuA in TFE and 338 NOEs (including 83 medium- and long-range NOEs) in DPC micelles were eventually employed for distance constraints. For both media, some correlations could not be assigned unambiguously and were included as restraints using a weighted average of the different possible distances which could make up the constraint (TFE, 22; DPC, 14). In both cases, eight hydrogen bonds detected by deuterium exchange experiments (CO_i-HN_{i+4}, range 1.8−2.2 Å, for $i = 19-26$) provided further restraints. Using distance geometry/simulated annealing calculations, a total of 20 and 25 structures for LeuA in TFE and DPC micelles,

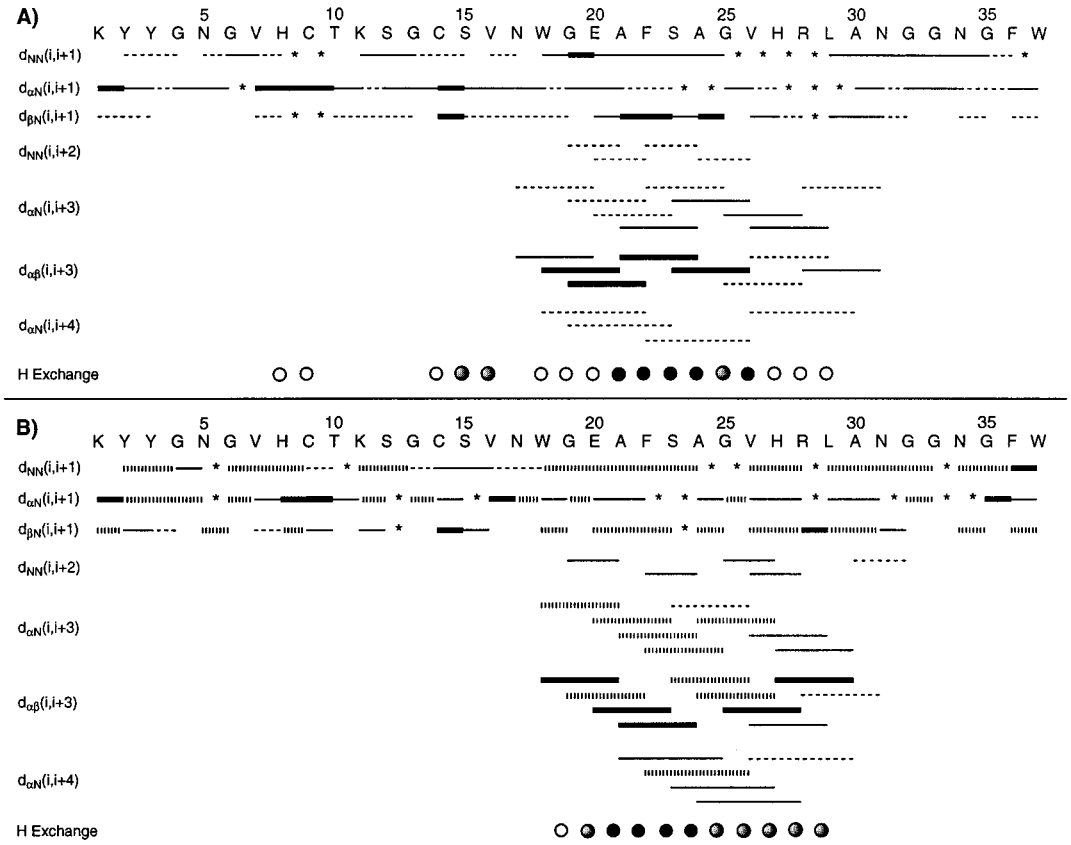

FIGURE 4: Pattern of interresidue NOEs observed at 150 ms mixing time for LeuA in (A) 90% TFE and (B) DPC micelles with relative intensities given by the bar thickness (thick line = strong, hashed line = medium strong, solid line = medium, and dashed line = weak). Asterisks (*) show areas where spectral overlap prevents unambiguous determination. Relative rates of amide hydrogen exchange (to ≥90%) are indicated as the last entry for each solvent by solid circles (≥24 h), half-filled circles (ca. 12−24 h), and open circles (ca. 3−12 h). Unmarked (no circle) residues exchange rapidly (≤3 h).

respectively, were generated. Of these 18 and 19 structures, respectively, had no distance violations greater than 0.25 Å.

The best fit superimposition of the backbone of the calculated structures with the lowest energies for LeuA in TFE based on different subsets of residues (7−30, 7−15, and 19−30) is shown in Figure 5A−C. An analogous set of superimposed structures for LeuA in DPC micelles is presented in Figure 5D−F. In TFE, most of the structure is well defined, including the β-sheet and α-helix described above, as indicated by the low average root mean square deviations (RMSD) in these domains (Table 1). More variability, presumably due to increased conformational averaging as evidenced by the smaller number of NOEs, is observed for the structures of LeuA in DPC micelles. However, in this medium, the α-helix is still very distinct. The N-terminal region is less well defined, but the β-sheet is still evident, especially around the disulfide loop. There appears to be more variability in the relationship between the α-helix and the β-sheet in DPC micelles. The first residues are much more disordered in DPC micelles than in TFE. To a lesser extent, the reverse is true for the C-terminus. These results are in agreement with the number of NOEs observed in the different regions for the two different media (Figure 4). The root mean square deviations for these LeuA structures are given in Table 1.

DISCUSSION

On the basis of what is known about the machinery involved in type IIa bacteriocin production and immunity, it is clear that a series of recognition events involving interaction between LeuA and other proteins must occur. These could include (1) specific export and processing of the initially synthesized preleucocin A by the ABC transporter-protease in conjunction with the membrane-bound accessory protein (van Belkum *et al.*, 1997, and references therein), (2) binding of LeuA to an unidentified receptor protein in the membrane of the target organism, and (3) protection of producing cells (and possibly resistant target cells) by the specific immunity protein (van Belkum & Stiles, 1995). Although the related carnobacteriocin B2 (Figure 1) shows little, if any, affinity for its immunity protein in solution (Quadri *et al.*, 1995), it may be that the putative receptor is involved in formation of a ternary complex with bacteriocin-immunity protein or that the appropriate membrane environment is essential for such interactions. Since a relatively complete bacteriocin structure appears essential for biological activity (Quadri *et al.*, 1994, 1997; Fleury *et al.*, 1996; see below), it seems reasonable that different domains in the sequence of LeuA must be able to adopt the appropriate conformation for effective binding to the various proteins. LeuA exists as a random coil in water and DMSO (Henkel *et al.*, 1992; Sailer *et al.*, 1993), but it is likely that upon initial interaction with the membrane of a producing or target cell it assumes an "active conformation" that assists its search and adhesion to the key proteins (Waterhous & Johnson, 1994; Moroder *et al.*, 1993; Schwyzer, 1995; Tessmer & Kallick, 1997). Primary goals of this study were to determine whether LeuA does assume defined conformations in mixed

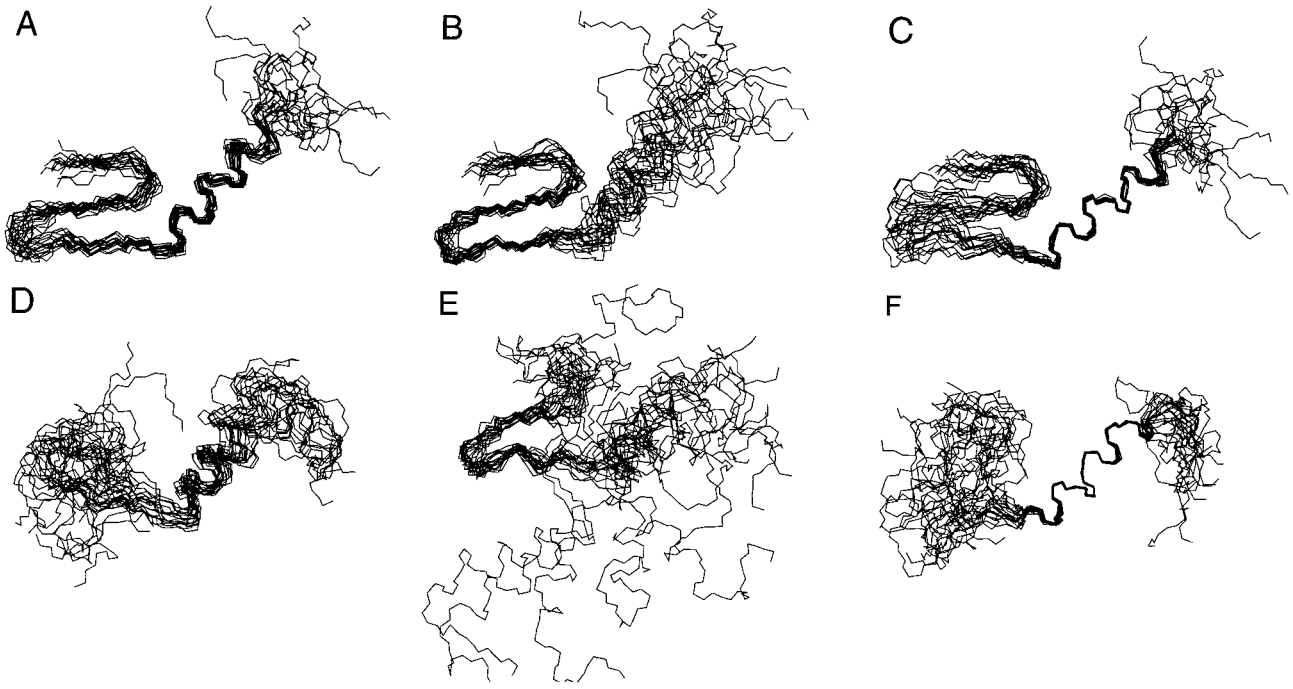

FIGURE 5: Superimposition of 18 calculated peptide backbone (N, C_α, CO) structures for LeuA in 90% TFE aligned for best overlap of residues (A) 7−30, (B) 7−15, and (C) 19−30. Comparable superimpositions of 19 structures for LeuA in DPC micelles are shown in (D)−(F).

Table 1: Root Mean Square Deviations (Å) for Leucocin A Structures

	TFE		DPC micelles		all	
residues	all atoms	backbone[a]	all atoms	backbone[a]	all atoms	backbone[a]
1−37	5.11	3.63	7.28	5.84	7.45	5.93
2−30	2.70	1.61	6.63	5.09	6.10	4.77
2−15	2.74	1.35	4.94	2.95	4.98	2.88
2−7	1.96	0.78	3.86	1.68	4.08	1.87
7−15	2.83	1.23	3.01	1.28	3.14	1.38
7−30	2.68	1.45	4.64	3.46	4.32	3.11
19−30	1.84	0.43	1.67	0.27	1.94	0.44
31−37	4.78	2.49	3.94	2.30	4.73	2.41

[a] Backbone atoms are defined as amide nitrogens and α and carbonyl carbons.

aqueous−lipophilic solvent systems and to identify spatial locations of amino acid residues that influence the biological effects of this type IIa bacteriocin.

The structures determined for LeuA in TFE and DPC micelles display a number of similarities. Figure 6 shows ribbon diagrams of the lowest energy structure for each medium superimposed for optimal overlap of the backbone of residues 19−30. The RMSD for the superimposition of all structures for various atom subsets is given in Table 1. The overall RMSD (all residues) is quite high (5.93 Å for backbone atoms), as expected due to the poor definition of the overall structure in DPC micelles. Even excluding the least defined atoms (residues 1, 31−37) does not greatly increase the fit. However, there is considerable similarity within different regions. The RMSD of 0.44 Å for residues 19−30 (backbone atoms only) clearly indicates that the α-helix region is well defined and essentially identical in the two different media. As mentioned above, this is in striking contrast to random coil structures seen in aqueous or DMSO environments (Henkel *et al.*, 1992; Sailer *et al.*, 1993). The β-sheet domain (2.88 Å; residues 2−15) also shows significant similarity for structures calculated for both TFE and DPC micelles. The agreement increases substantially when smaller sections of this region are compared in the two solvents.

These facts indicate that certain structural features (i.e., α-helix and three-strand antiparallel β-sheet) are present in the conformations LeuA adopts in the two media but that the orientation between the different regions is variable. The differences between the two sets of structures most likely reflect altered population levels for certain conformers between the two types of conditions used. However, the structure of LeuA is probably averaged over the whole set of conformers. In TFE, the β-sheet region is restricted to a smaller set of conformers on the basis of a few weak NOEs (see above). Similarly, the C-terminus in DPC is somewhat better defined because of a few restraints placed on its orientation. The use of these NOEs, in both cases, may overemphasize certain conformers.

Examination of the helical portions indicates that hydrophobic residues appear on one surface in both solvents, whereas the hydrophilic residues occupy the opposite side, typical of an amphiphilic helix (Figure 7). Closer inspection of the helical region shows that the side chains of Trp18, Phe22, Val26, and Leu29 form a defined and compact hydrophobic surface on one side of the helix. The hydrophilic side chains of Asn17, Glu20, His27, Arg28, and Asn31 appear on the opposite side. Mes has been suggested to form an analogous amphipathic α-helix on the basis of a CD study (Fleury *et al.*, 1996). The two residues which differ between Mes and LeuA (22 and 26) both appear in close proximity on the hydrophobic side of the helix. Preliminary NMR studies of carnobacteriocin B2 suggest that it also possesses an α-helix between residues 17 and 39 (N. L. F. Gallagher, and J. C. Vederas, unpublished results).

This amphipathic helix is likely to be very important for the biological activity for LeuA, possibly by interaction with a lipophilic region on the receptor protein. Although the

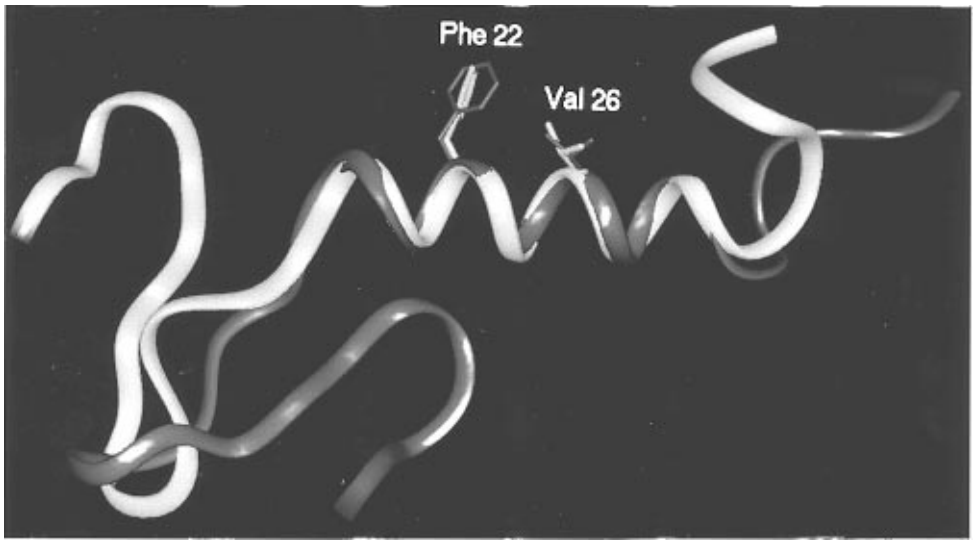

FIGURE 6: Superimposition of ribbon diagrams of the lowest energy LeuA structures in 90% TFE (blue) and DPC micelles (pink) aligned for best overlap of the α-helix region.

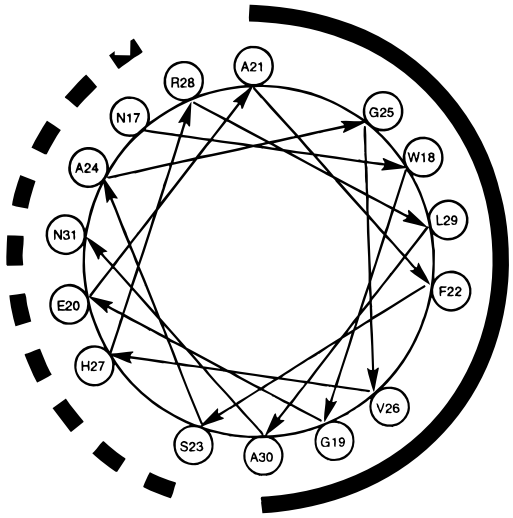

FIGURE 7: Edmundson α-helical wheel representation of residues 17−31 of LeuA. The solid curve indicates hydrophobic amino acids and the dashed curve denotes hydrophilic residues.

"YGNGV" bacteriocins possess a large amount of homology (Figure 1), they show different specificities in terms of antimicrobial activity which cannot be explained by a simple aggregation and membrane pore formation model. This indicates that at least one key molecular recognition event must occur for antimicrobial activity, most likely binding to a membrane-bound receptor protein. Recent experiments with lactococcin A (van Belkum *et al.*, 1991; Abee, 1995b), another class II bacteriocin (Klaenhammer, 1993), indicate that a such a protein may be critical for the antimicrobial action of such compounds. A similar receptor has been suggested by studies on the mode of action of pediocin PA-1 (Chikindas *et al.*, 1993).

As the N-terminal sections (residues 1−21) of many type IIa bacteriocins are highly conserved and the C-terminal domains (residues 22+) are much more diverse, it appears that the differences in sensitivity of target bacteria are determined by receptor recognition of the C-terminal region of these peptides. This observation is supported by a recent report wherein four hybrid bacteriocins were constructed with the first 21 residues of one bacteriocin sequence attached to the C-terminus of another (Fimland *et al.*, 1996). These hybrid peptides (pediocin−sakacin P, sakacin P−pediocin, curvacin A−sakacin P, sakacin P−curvacin A) were all bactericidal and displayed an antimicrobial spectrum corresponding to that of the parent having the same C-terminus. The location of the Phe22 and Val26 side chains in the α-helix of the three-dimensional structural model of LeuA (Figure 7) supports the attractive hypothesis that they may form part of a hydrophobic recognition surface for a receptor, thereby accounting for slight differences in the antimicrobial spectrum (Héchard *et al.*, 1992; Fremaux *et al.*, 1995) relative to mesentericin Y105 (Mes). However, work by our group on carnobacteriocin B2 (Quadri *et al.*, 1994, 1997) and a report on Mes analogs (Fleury *et al.*, 1996) indicate that the entire structure of such bacteriocins is necessary for antimicrobial action. Large fragments derived from selective cleavage of carnobacteriocin B2 display no activity (Quadri *et al.*, 1994). Removal from Mes of either the first three N-terminal residues or the C-terminal Trp37 results in a drastic reduction in activity against *Listeria ivanovii* (Fleury *et al.*, 1996). The latter authors suggest that the first 14 residues of Mes at the N-terminus, as opposed to the α-helix, are involved in the receptor recognition event but offer no proof other than loss of activity against a single organism. Although it may also be involved in the receptor-binding event, the N-terminal region, with its conserved YGNGV motif, is likely to dominate a different aspect in the mechanism of action that is common to all of these bacteriocins. Our recent work on carnobacteriocin B2 mutants has shown that, while conservative changes (e.g., Ile for Val) in amino acids in its putative α-helical region have no significant effect on activity against *C. divergens*, replacement of Phe33 by serine in this domain results in complete loss of activity (Quadri *et al.*, 1997). This change may affect the amphiphilicity of the α-helix, as reflected in greatly altered HPLC retention times. Also, replacement of Tyr3 (part of the YGNGV conserved N-terminal domain) with phenylalanine (i.e., substitution of OH by H) in the first β-sheet drastically reduced the antimicrobial activity. In contrast, acylation with biotin of one of the ϵ-amino groups of the two lysines (residues 1 and 11) in LeuA with consequent loss of positive charge does not significantly decrease the activity against a test strain, *C. divergens* (Y.-

Z. Yan, and J. C. Vederas, unpublished results). The emerging picture is that the β-sheet loop exercises an important effect common to this class of bacteriocins whereas the α-helical part determines target specificity (i.e., antimicrobial spectrum) through receptor binding but that correct spatial arrangement of key amino acid side chains in both sections is essential.

Although the disulfide bridge clearly helps to provide a more defined structure to the N-terminal domain of LeuA, its exact biological function is still uncertain. Jack *et al.* (1995) have suggested that there is a correlation between the cysteine content of non-lanthionine-containing bacteriocins and their spectrum of antibacterial activity, with those containing two or more cysteines having the broadest spectrum of bioactivity. However, carnobacteriocin B2 does not appear to readily form a disulfide bridge, even though it contains two cysteines at the same positions on the peptide chain (Quadri *et al.*, 1994). In contrast, analogs of Mes wherein the cysteines were replaced with either serines or acetamidomethylcysteines which cannot form disulfide bonds resulted in reduction of bioactivity by factors of 20 000 and 2500, respectively (Fleury *et al.*, 1996). Interestingly, both of these analogs showed reduced amounts of α-helix formation in TFE as demonstrated by CD spectra, thereby suggesting interaction between the different domains of the peptide. The activity of pediocin PA-1/AcH is decreased (Jack *et al.*, 1995) or lost (Chikindas *et al.*, 1993) by heating with either dithiothreitol or β-mercaptoethanol. However, this peptide has two disulfide bonds (between Cys9 and Cys14 and between Cys24 and Cys44). Thus it is unclear whether the reduction of one or both disulfide bridges is responsible for the loss of activity. It should be noted that the second of these causes the C-terminus to be folded back on the region analogous to the α-helix in LeuA. The structure of LeuA in DPC micelles shows a similar effect (Figure 6). Interpretation of the significance of this requires identification of receptors and a detailed understanding of the bacteriocin−protein interactions, but it can be observed that pediocin PA-1/AcH has a broader spectrum of activity than LeuA (Jack *et al.*, 1995).

Bacteriocins of lactic acid bacteria, including LeuA (Hastings *et al.*, 1991; Felix *et al.*, 1994), are initially synthesized as prebacteriocins having a leader peptide which is removed by proteolytic processing, frequently following a Gly-Gly site [for a discussion of bacteriocin leader peptides and secretion, see Worobo *et al.* (1995) and van Belkum *et al.* (1997); for a discussion of other genes involved in production and immunity to class II bacteriocins, see Axelsson and Holck (1994)]. Preleucocin has recently been overexpressed and shown to have little, if any, antimicrobial activity (M. van Belkum, and M. E. Stiles, unpublished results). Also, carnobacteriocin B2 is 125 times more active than its corresponding prepeptide, precarnobacteriocin B2 (Quadri *et al.*, 1997). Hence, it is tempting to speculate that the leader peptide not only assists in the transport of the bacteriocin to the exterior of the producing cell but also conformationally interferes with exposure of the surface(s) required for antimicrobial activity. Our work shows that processed mature bacteriocin, LeuA, exists as a random coil after export to the medium (water) but assumes a defined conformation upon interaction with environments which mimic the lipophilicity that would be found in the membrane of a target organism. Like other bacteriocins, LeuA has a narrow spectrum of activity relative to other classes of antibiotics, possibly because of structural demands for recognition by specific receptor proteins in the membranes of sensitive bacteria, such as the potential pathogen, *Listeria monocytogenes.* Immunity proteins generated within bacteriocin-producing organisms appear to show little direct binding to the bacteriocin (Quadri *et al.*, 1995) but may act as allosteric inhibitors of the bacteriocin−receptor interaction. The present work, which describes the first experimental determination of the solution structure of a type IIa lactic acid bacteriocin, provides an experimental basis to test these ideas. Additional studies on the three-dimensional structures of preleucocin A as well as of other bacteriocins and their immunity proteins will be reported in due course. Experiments to identify the key bacteriocin receptor are in progress.

ACKNOWLEDGMENT

The authors thank Professor Cyril M. Kay and Mr. Kim Oikawa for acquisition of CD data (Biochemistry Department, University of Alberta). Dr. Laird Trimble (Merck Frosst Ltd., Pointe Claire, Quebec) is gratefully acknowledged for helpful suggestions and a generous gift of perdeuterated dodecylphosphocholine (DPC-d_{38}).

SUPPORTING INFORMATION AVAILABLE

Eight tables of ^{1}H chemical shifts of leucocin A in TFE and DPC micelles and distance restraints used for structure calculations (19 pages). Ordering information is given on any current masthead page.

REFERENCES

Abee, T. (1995a) *FEMS Microbiol. Lett. 129*, 1−10.

Abee, T. (1995b) *Workshop on the Bacteriocins of Lactic Acid Bacteria*, Abstract 5.2, Banff Conference Centre, Banff, Alberta.

Axelsson, L., & Holck, A. (1994) *J. Bacteriol. 177*, 2125−2137.

Bax, A. (1994) *Curr. Opin. Struct. Biol. 4*, 738−744.

Bhugaloo-Vial, P., Dousset, X., Metivier, A., Sorokine, O., Anglade, P., Boyaval, P., & Marion, D. (1996) *Appl. Environ. Microbiol. 62*, 4410−4416.

Brahms, S., & Brahms, J. (1980) *J. Mol. Biol. 138*, 149−178.

Brown, L. R., & Wüthrich, K. (1981) *Biochim. Biophys. Acta 647*, 95−111.

Bruno, M. C., & Montville, T. J. (1993) *Appl. Environ. Microbiol. 59*, 3003−3010.

Bukhtiyarova, M., Yang, R., & Ray, B. (1994) *Appl. Environ. Microbiol. 60*, 3405−3408.

Chang, C. T., Wu, C.-S. C., & Yang, J. T. (1978) *Anal. Biochem. 91*, 13−31.

Chen, Y., Shapira, R., Eisenstein, M., & Montville, T. J. (1997) *Appl. Environ. Microbiol. 63*, 1−8.

Chikindas, M. L., García-Garcerá, M. J., Driessen, A. J. M., Ledeboer, A. M., Nissen-Meyer, J., Nes, I. F., Abee, T., Konings, W. N., & Venema, G. (1993) *Appl. Environ. Microbiol. 59*, 3577−3584.

Christensen, D. P., & Hutkins, R. W. (1994) *Appl. Environ. Microbiol. 60*, 3870−3873.

Constantine, K. L., Mapelli, C., Meyers, C. A., Friedrichs, M. S., Krystek, S., & Mueller, L. (1993) *J. Biol. Chem. 268*, 22830−22837.

Dauber-Osguthorpe, P., Roberts, V. A., Osguthorpe, D. J., Wolff, J., Genest, M., & Hagler, A. T. (1988) *Proteins: Struct. Funct., Genet. 4*, 31−47.

Edison, A. S., Abildgaard, F., Westler, W. M., Mooberry, E. S., & Markley, J. L. (1994) *Methods Enzymol. 239*, 3−79.

Engelke, G., Gutowski-Eckel, Z., Kiesau, P., Siegers, K., Hammelmann, M., & Entian, K. D. (1994) *Appl. Environ. Microbiol. 60*, 814−825.

Felix, J. V., Papathanasopoulos, M. A., Smith, A. A., von Holy, A., & Hastings, J. W. (1994) *Curr. Microbiol. 29*, 207−212.
Fimland, G., Blingsmo, O. R., Sletten, K., Jung, G., Nes, I. F., & Nissen-Meyer, J. (1996) *Appl. Environ. Microbiol. 62*, 3313−3318.
Fleury, Y., Dayem, M. A., Montagne, J. J., Chabiosseau, E., Le Caer, J. P., Nicolas, P., & Delfour, A. (1996) *J. Biol. Chem. 271*, 14421−14429.
Franke, C. M., Leenhouts, K. J., Haandrikman, A. J., Kok, J., Venema, G., & Venema, K. (1996) *J. Bacteriol. 178*, 1766−1769.
Fremaux, C., Héchard, Y., & Cenatiempo, Y. (1995) *Microbiology (London) 141*, 1637−1645.
Griesinger, C., Otting, G., Wüthrich, K., & Ernst, R. R. (1988) *J. Am. Chem. Soc. 110*, 7870-7872.
Hastings, J. W., Sailer, M., Johnston, K., Roy, K. L., Vederas, J. C., & Stiles, M. E. (1991) *J. Bacteriol. 173*, 7491−7500.
Hastings, J. W., Stiles, M. E., & von Holy, A. (1994) *Int. J. Food Microbiol. 24*, 75−81.
Havel, T. F. (1991) *Prog. Biophys. Mol. Biol. 56*, 43−78.
Héchard, Y., Dérijard, B., Letellier, F., & Cenatiempo, Y. (1992) *J. Gen. Microbiol. 138*, 2725−2731.
Henkel, T., Sailer, M., Helms, G. L., Stiles, M. E., & Vederas, J. C. (1992) *J. Am. Chem. Soc. 114*, 1898−1900.
Holck, A., Axelsson, L., Birkeland, S.-E., Aukrust, T., & Blom, H. (1992) *J. Gen. Microbiol. 138*, 2715−2720.
Holck, A., Axelsson, L., Hühne, K., & Kröckel, L. (1994) *FEMS Microbiol. Lett. 115*, 143−150.
Hoover, D. J., & Steenson, L. R., Eds. (1993) *Bacteriocins of Lactic Acid Bacteria*, Academic Press, San Diego.
Inagaki, F., Shimada, I., Kawaguchi, K., Hirano, M., Terasawa, I., Ikura, T., & Go, N. (1989) *Biochemistry 28*, 5985−5991.
Jack, R. W., Tagg, J. R., & Ray, B. (1995) *Microbiol. Rev. 59*, 171−200.
Jasanoff, A., & Fersht, A. R. (1994) *Biochemistry 33*, 2129−2135.
Jeener, J., Meier, B. H., Bachmann, P., & Ernst, R. R. (1979) *J. Chem. Phys. 71*, 4546−4553.
Jung, G., & Sahl, H. G., Eds. (1991) *Nisin and Novel Lantibiotics*, ESCOM Science Publishers, Leiden, The Netherlands.
Kaiser, A. L., & Montville, T. J. (1996) *Appl. Environ. Microbiol. 62*, 4529−4535.
Kallick, D. A. (1993) *J. Am. Chem. Soc. 115*, 9317−9318.
Karslake, C., Piotto, M. E., Pak, Y. K., Weiner, H., & Gorenstein, D. G. (1990) *Biochemistry 29*, 9872−9878.
Klaenhammer, T. R. (1993) *FEMS Microbiol. Rev. 12*, 39−86.
Kuipers, O. P., Beerthuyzen, M. M., Siezen, R. J., & De Vos, W. M. (1993) *Eur. J. Biochem. 216*, 281−291.
Leopold, M. F., Urbauer, J. L., & Wand, A. J. (1994) *Mol. Biotechnol. 2*, 61−93.
Macquaire, F., Baleux, F., Giaccobi, E., Huyn-Dinh, T., Neumann, J.-M., & Sanson, A. (1992) *Biochemistry 31*, 2576−2582.
Maftah, A., Renault, D., Vignoles, C., Héchard, Y., Bressollier, P., Ratinaud, M. H., Cenatiempo, Y., & Julien, R. (1993) *J. Bacteriol. 175*, 3232−3235.
Marugg, J. D., Gonzalez, C. F., Kunka, B. S., Ledeboer, A. M., Pucci, M. J., Toonen, M. Y., Walker, S. A., Zoetmulder, L. C. M., & Vandenbergh, P. A. (1992) *Appl. Environ. Microbiol. 58*, 2360−2367.
Merutka, G., Dyson, H. J., & Wright, P. E. (1995) *J. Biomol. NMR 5*, 14−24.
Montville, T. J., & Bruno, M. E. C. (1994) *Int. J. Food Microbiol. 24*, 53−74.
Moroder, L., Romano, R., Guba, W., Mierke, D. F., Kessler, H., Delporte, C., Winand, J., & Christophe, J. (1993) *Biochemistry 32*, 13551−13559.
Motlagh, A., Bukhtiyarova, M., & Ray, B. (1994) *Lett. Appl. Microbiol. 18*, 305−312.
Nissen-Meyer, J., & Nes, I. F. (1997) *Arch. Microbiol. 167*, 66−77.
Quadri, L. E. N., Sailer, M., Roy, K. L., Vederas, J. C., & Stiles, M. E. (1994) *J. Biol. Chem. 269*, 12204−12211.
Quadri, L. E. N., Sailer, M., Terebiznik, M. R., Roy, K. L., Vederas, J. C., & Stiles, M. E. (1995) *J. Bacteriol. 177*, 1144−1151.
Rance, M., Sørenson, O. W., Bodenhausen, G., Wagner, G., Ernst, R. R., & Wüthrich, K. (1983) *Biochem. Biophys. Res. Commun. 117*, 479−485.
Roberts, G. C. K., Ed. (1993) *NMR of Macromolecules, a Practical Approach*, Oxford University Press, Oxford.
Saberwal, G., & Nagaraj, R. (1994) *Biochim. Biophys. Acta 1197*, 109−131.
Sailer, M., Helms, G. L., Henkel, T., Niemczura, W. P., Stiles, M. E., & Vederas, J. C. (1993) *Biochemistry 32*, 310−318.
Schwyzer, R. (1986) *Biochemistry 25*, 6335−6350.
Stiles, M. E. (1994) *J. Dairy Sci. 77*, 2718−2724.
Stiles, M. E. (1996) *Antoine van Leeuwenhoek 70*, 331−345.
Tessmer, M. R., & Kallick, D. A. (1997) *Biochemistry 36*, 1971−1981.
Thornton, K., & Gorenstein, D. G. (1994) *Biochemistry 33*, 3532−3539.
Thornton, K., Wang, Y., Weiner, H., & Gorenstein, D. G. (1993) *J. Biol. Chem. 268*, 19906-19914.
Tichaczek, P. S., Vogel, R. F., & Hammes, W. P. (1993) *Arch. Microbiol. 160*, 279−283.
Tichaczek, P. S., Vogel, R. F., & Hammes, W. P. (1994) *Microbiology (London) 140*, 361−367.
van Belkum, M. J., & Stiles, M. E. (1995) *Appl. Environ. Microbiol. 61*, 3573−3579.
van Belkum, M. J., Kok, J., Venema, G., Holo, H., Nes, I. F., Konings, W. N., & Abee, T. (1991) *J. Bacteriol. 173*, 7934−7941.
van Belkum, M. J., Worobo, R. W., & Stiles, M. E. (1997) *Mol. Microbiol. 23*, 1293−1301.
van den Hooven, H. W., Fogolari, F., Rollema, H. S., Konings, R. N. H., Hilbers, C. W., & van de Ven, F. J. M. (1993) *FEBS Lett. 319*, 189−194.
van den Hooven, H. W., Henno W., Spronk, C. A. E. M., van de Kamp, M., Konings, R. N. H., Hilbers, C. W., & van de Ven, F. J. M. (1996) *Eur. J. Biochem. 235*, 394−403.
Waterhous, D. V., & Johnson, W. C., Jr. (1994) *Biochemistry 33*, 2121−2128.
Wider, G., Lee, K. H., & Wüthrich, K. (1982) *J. Mol. Biol. 155*, 367−388.
Wishart, D. S., & Sykes, B. D. (1994) *Methods Enzymol. 239*, 363−392.
Worobo, R. W., van Belkum, M. J., Sailer, M., Roy, K. L., Vederas, J. C., & Stiles, M. E. (1995) *J. Bacteriol. 177*, 3143−3149.
Wüthrich, K. (1986) *NMR of Proteins and Nucleic Acids*, John Wiley & Sons, New York.

BI971263H